A Distributed Optimization Method for Spacecraft Attitude Control and Vibration Suppression

Yabo Hu*
Harbin Institute of Technology, Harbin 150001, People's Republic of China

Franco Bernelli-Zazzera†
Politecnico di Milano, 20156, Milano, Italy

Yunhai Geng‡
Harbin Institute of Technology, Harbin 150001, People's Republic of China

I. Introduction

To achieve high-precision attitude control, vibration suppression is required for large spacecraft. The actuators for attitude control and/or vibration suppression can be installed centralized or distributed. In the former case, some vibration suppression methods are based on trajectory planning [1, 2], while others are integrated in attitude control law [3]. The capabilities of these methods for vibration suppression are limited due to their open-loop design-based attribution or lack of dedicated actuators for vibration suppression. Hence, attitude control and vibration suppression based on distributed actuators are becoming a research hotspot.

Various types of actuator have been scattered across the spacecraft for vibration suppression, including piezoelectric actuators (PZTs) [4, 5] and control moment gyroscopes (CMGs) [6–13]. The concept of angular momentum being studied as a distributed parameter was first introduced by D'Eleuterio and Hughes [6, 7]. By importing infinitesimal angular momentum devices to the elastic body, the frequencies, coupled modes, and damping can be controlled. To facilitate engineering application, Hu et al. [10–13] proposed a practical methodology for active vibration suppression and attitude control of flexible structures by CMGs. In Hu's studies, the angular momentum is discretely distributed in the structure rather than continuously [6, 7]. According to the model in [11], Guo et al. proposed a modal force compensator method [14] and a null-motion based method [15] to suppress vibration. Different from the idea of designing the control law and the steering law of actuators together [10–15], Hu et al. [16, 17] proposed two control law design methods for attitude control and vibration suppression. The advantage is that the proposed methods can be used for systems with different kinds of actuators.

The aforementioned methods are all centralized. Even in [17] the proposed control allocation based method can be implemented in a distributed way, it still needs a central unit to calculate the ideal torque. The same distribution also appeared in [18] and [19]. This distribution is not thorough in some senses. Moreover, many of the methods mentioned

*Ph.D candidate, Research Center of Satellite Technology; huyabo@hit.edu.cn.
†Full professor, Department of Aerospace Science and Technology; franco.bernelli@polimi.it. Sinior Member AIAA.
‡Professor, Research Center of Satellite Technology; gengyh@hit.edu.cn.

above only realize the attitude control and vibration suppression functions of flexible spacecraft, and do not achieve the optimization of certain objectives [10–16]. These design methods are relatively conservative.

Motivated by [20] and [21], a distributed optimization method for flexible spacecraft attitude control and vibration suppression is proposed. Firstly, it is necessary to formulate the problem into a standard optimization problem. In this process, the design methods of attitude control law and objective function of the optimization problem are proposed. To realize thoroughly distributed computing, the main idea here is to assume that each actuator node adopts the same form of control law, and the parameters of the control law at each node are obtained by a distributed optimization method. The dynamic and steady-state performance of the system is characterized by equality constraints including parameters of all actuators. To meet these global equality constraints, surplus variables are introduced to each actuator. In this way, each actuator solves the KKT (Karush-Kuhn-Tucker) conditions related to the surplus variables. When all surplus variables converge to zero, all actuators obtain the optimal solution. This is the core difference of distribution between the proposed method here and the methods in previous [17–19]. Ideal control torque by central calculation unit is not needed in the method proposed in this paper. In addition, we also give a method to deal with the coupling constraints of local variables, which can not be handled by the methods in [19] and [21].

II. System Description

The system considered here is a free-flying flexible structure with distributed angular momentum exchange actuators (reaction wheels and/or CMGs), as shown in Fig.1. $A_i,\ i = 1, \cdots, n$ represent the actuator mounting nodes.

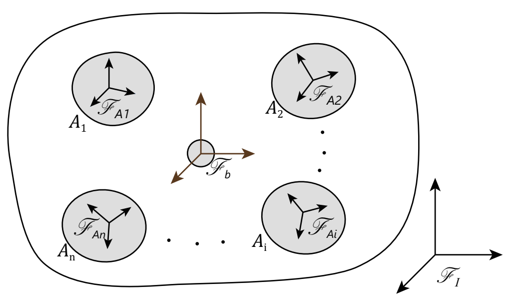

Fig. 1 Model of flexible spacecraft with distributed actuators.

Since the modeling of the rotational and elastic dynamics of the unconstrained flexible spacecraft with momentum exchange actuators has been well studied in the previous literature [10–13], the dynamics equations are directly stated here as follows, where the elastic motion of the structure is assumed to be small [11].

$$\boldsymbol{J}\dot{\omega} + \omega \times \boldsymbol{J}\omega + \boldsymbol{M}\ddot{\boldsymbol{\eta}} - \sum_{i=1}^{n} \boldsymbol{h}_i \times \omega - \sum_{i=1}^{n} \boldsymbol{h}_i \times \dot{\boldsymbol{\beta}}_i = \boldsymbol{T}_c + \boldsymbol{T}_d \tag{1a}$$

$$\ddot{\boldsymbol{\eta}} + \boldsymbol{E}\dot{\boldsymbol{\eta}} + \boldsymbol{K}\boldsymbol{\eta} + \boldsymbol{M}^{\mathrm{T}}\dot{\omega} - \sum_{i=1}^{n} \boldsymbol{R}_i^{\mathrm{T}}\boldsymbol{h}_i \times (\omega + \dot{\boldsymbol{\beta}}_i) = \boldsymbol{T}_e \tag{1b}$$

where $\boldsymbol{\omega} \in \mathbb{R}^3$ denotes the body angular velocity of the spacecraft with respect to the inertial frame $\mathscr{F}_I$ and is expressed in the body frame $\mathscr{F}_b$. $\boldsymbol{J} \in \mathbb{R}^{3\times3}$ represents the total moment of inertia of the undeformed spacecraft; $\boldsymbol{M} \in \mathbb{R}^{3\times m}$ represents the modal angular momentum coefficient matrix and m is the number of the considered elastic modes. $\boldsymbol{h}_i$ denotes the total angular momentum of each actuator mounting node A_i, respectively. $\boldsymbol{\eta} \in \mathbb{R}^m$ is the generalized coordinate vector for the elastic displacement. $\boldsymbol{E} = \mathrm{diag}(2\xi_i w_i),\ i = 1, \cdots, m$, denotes the damping matrix; $\boldsymbol{K} = \mathrm{diag}(w_i^2),\ i = 1, \cdots, m$, represents the stiffness matrix; ξ_i and w_i represent damping coefficients and natural frequencies, respectively. $\boldsymbol{\beta}_i = \boldsymbol{R}_i\boldsymbol{\eta},\ i = 1, \cdots, n$, is the rotational displacement of the node A_i, and $\boldsymbol{R}_i$ denotes the rotational modal matrix, which is obtained from the finite element method in engineering. Note that $\dot{\boldsymbol{\beta}}_i = \boldsymbol{\omega}_i - \boldsymbol{\omega}$ is measurable, in which $\boldsymbol{\omega}_i$ is the inertial angular velocity of the node A_i with respect to the inertial frame $\mathscr{F}_I$ and expressed in the body frame $\mathscr{F}_b$. $\boldsymbol{T}_d$ is the vector of external disturbances. The quantities representing the attitude control torques $\boldsymbol{T}_c$ and modal forces $\boldsymbol{T}_e$ generated by all actuators can be expressed as

$$\boldsymbol{T}_c = \sum_{i=1}^{n} \boldsymbol{T}_i; \quad \boldsymbol{T}_e = \sum_{i=1}^{n} \boldsymbol{R}_i^{\mathrm{T}} \boldsymbol{T}_i \tag{2}$$

where $\boldsymbol{T}_i$ is the total torque produced at node A_i.

The quaternion parameter is employed to describe the attitude kinematics of spacecraft

$$\dot{q}_0 = -\frac{1}{2}\boldsymbol{q}^{\mathrm{T}}\boldsymbol{\omega} \tag{3a}$$

$$\dot{\boldsymbol{q}} = \frac{1}{2}\left(q_0\boldsymbol{I}_3 + \boldsymbol{q}^{\times}\right)\boldsymbol{\omega} \tag{3b}$$

where $\left[q_0, \boldsymbol{q}^{\mathrm{T}}\right]^{\mathrm{T}}$ is the quaternion vector from the body frame $\mathscr{F}_b$ to the inertial frame $\mathscr{F}_I$ satisfying normalization contraint $q_0^2 + \boldsymbol{q}^{\mathrm{T}}\boldsymbol{q} = 1$, $q_0 \in \mathbb{R}$ and $\boldsymbol{q} = [q_1,\ q_2,\ q_3]^{\mathrm{T}} \in \mathbb{R}^3$ denote the scalar and vector components of the quaternion vector, respectively. $\boldsymbol{I}_3$ is 3×3 identity matrix. $\boldsymbol{q}^{\times} \in \mathbb{R}^{3\times3}$ is a skew-symmetric matrix satisfying $\boldsymbol{a} \times \boldsymbol{b} = \boldsymbol{a}^{\times}\boldsymbol{b}$ for vectors $\boldsymbol{a}, \boldsymbol{b} \in \mathbb{R}^3$.

III. Design of Control Law

To facilitate the design of control law and the analysis of its stability, the above dynamics model Eq.(1) can be rewritten in a compact form [15]

$$\bar{\boldsymbol{M}}\ddot{\boldsymbol{v}} + \left(\bar{\boldsymbol{G}} + \bar{\boldsymbol{E}}\right)\dot{\boldsymbol{v}} + \bar{\boldsymbol{K}}\boldsymbol{v} = \boldsymbol{f} \tag{4}$$

where

$$\bar{\boldsymbol{M}} = \begin{bmatrix} \boldsymbol{J} & \boldsymbol{M} \\ \boldsymbol{M}^{\mathrm{T}} & \boldsymbol{I} \end{bmatrix},\ \bar{\boldsymbol{G}} = \begin{bmatrix} \boldsymbol{G}_{rr} & \boldsymbol{G}_{re} \\ -\boldsymbol{G}_{re}^{\mathrm{T}} & \boldsymbol{G}_{ee} \end{bmatrix},\ \bar{\boldsymbol{E}} = \begin{bmatrix} \boldsymbol{0} & \boldsymbol{0} \\ \boldsymbol{0} & \boldsymbol{E} \end{bmatrix},\ \bar{\boldsymbol{K}} = \begin{bmatrix} \boldsymbol{0} & \boldsymbol{0} \\ \boldsymbol{0} & \boldsymbol{K} \end{bmatrix} \tag{5}$$

$$\boldsymbol{v} = \begin{bmatrix} \boldsymbol{\theta} \\ \\ \boldsymbol{\eta} \end{bmatrix}, \quad \boldsymbol{f} = \begin{bmatrix} \boldsymbol{T}_c + \boldsymbol{T}_d - \boldsymbol{\omega} \times \boldsymbol{J}\boldsymbol{\omega} \\ \\ \boldsymbol{T}_e \end{bmatrix} \tag{6}$$

in which $\boldsymbol{G}_{rr} = -\sum_{i=1}^{n} \boldsymbol{h}_i^{\times}$ and $\boldsymbol{G}_{ee} = -\sum_{i=1}^{n} \boldsymbol{R}_i^{\mathrm{T}} \boldsymbol{h}_i^{\times} \boldsymbol{R}_i$ are skew-symmetric matrices, $\boldsymbol{G}_{re} = -\sum_{i=1}^{n} \boldsymbol{h}_i^{\times} \boldsymbol{R}_i$. Thus, $\bar{\boldsymbol{G}}$ is a skew-symmetric matrix too; $\boldsymbol{\theta}$ is defined as $\dot{\boldsymbol{\theta}} = \boldsymbol{\omega}$.

Since the main focus of this paper is the distributed design and implementation of algorithm among the actuators, a simple form of control law is chosen for each actuator

$$\boldsymbol{T}_i = -k_{pi}\boldsymbol{q} - k_{di}\boldsymbol{\omega}_i, \ i = 1, \cdots, n \tag{7}$$

where k_{pi} and k_{di} are positive control gains. The following Lyapunov function is chosen for stability analysis, in which the external disturbances $\boldsymbol{T}_d$ is omitted [15]

$$V = \sum_{i=1}^{n} k_{pi} \left[(1 - q_0)^2 + \boldsymbol{q}^{\mathrm{T}}\boldsymbol{q} \right] + \frac{1}{2}\dot{\boldsymbol{v}}^{\mathrm{T}}\bar{\boldsymbol{M}}\dot{\boldsymbol{v}} + \frac{1}{2}\boldsymbol{v}^{\mathrm{T}}\bar{\boldsymbol{K}}\boldsymbol{v} \geq 0 \tag{8}$$

The time derivation of Eq.(8) can be written as

$$\begin{aligned} \dot{V} &= \sum_{i=1}^{n} k_{pi}\boldsymbol{q}^{\mathrm{T}}\boldsymbol{\omega} + \dot{\boldsymbol{v}}^{\mathrm{T}} \left[-\left(\bar{\boldsymbol{G}} + \bar{\boldsymbol{E}}\right)\dot{\boldsymbol{v}} + \boldsymbol{f} \right] \\ &= \sum_{i=1}^{n} k_{pi}\boldsymbol{q}^{\mathrm{T}}\boldsymbol{\omega} - \dot{\boldsymbol{\eta}}^{\mathrm{T}}\boldsymbol{E}\dot{\boldsymbol{\eta}} + \boldsymbol{\omega}^{\mathrm{T}}\boldsymbol{T}_c + \dot{\boldsymbol{\eta}}^{\mathrm{T}}\boldsymbol{T}_e \end{aligned} \tag{9}$$

Substituting Eq.(2) and Eq.(7) into the above equation yields

$$\begin{aligned} \dot{V} &= \sum_{i=1}^{n} k_{pi}\boldsymbol{q}^{\mathrm{T}}\boldsymbol{\omega} + \sum_{i=1}^{n} \boldsymbol{\omega}_i^{\mathrm{T}}(-k_{pi}\boldsymbol{q} - k_{di}\boldsymbol{\omega}_i) - \dot{\boldsymbol{\eta}}^{\mathrm{T}}\boldsymbol{E}\dot{\boldsymbol{\eta}} \\ &= -\sum_{i=1}^{n} k_{pi}\dot{\boldsymbol{\beta}}_i^{\mathrm{T}}\boldsymbol{q} - \sum_{i=1}^{n} k_{di}\boldsymbol{\omega}_i^{\mathrm{T}}\boldsymbol{\omega}_i - \dot{\boldsymbol{\eta}}^{\mathrm{T}}\boldsymbol{E}\dot{\boldsymbol{\eta}} \end{aligned} \tag{10}$$

According to the Young's inequality with ϵ, $-k_{pi}\dot{\boldsymbol{\beta}}_i^{\mathrm{T}}\boldsymbol{q} \leq k_{pi}\dot{\boldsymbol{\beta}}_i^{\mathrm{T}}\dot{\boldsymbol{\beta}}_i\boldsymbol{q}^{\mathrm{T}}\boldsymbol{q}\epsilon_i/2 + k_{pi}/(2\epsilon_i)$, where ϵ_i is the parameter in the Young's inequality. The inequality is valid for every $\epsilon_i > 0$. Then,

$$\begin{aligned} \dot{V} &\leq \sum_{i=1}^{n} k_{pi}\frac{\dot{\boldsymbol{\beta}}_i^{\mathrm{T}}\dot{\boldsymbol{\beta}}_i\boldsymbol{q}^{\mathrm{T}}\boldsymbol{q}\epsilon_i}{2} - \sum_{i=1}^{n} k_{di}\boldsymbol{\omega}_i^{\mathrm{T}}\boldsymbol{\omega}_i - \dot{\boldsymbol{\eta}}^{\mathrm{T}}\boldsymbol{E}\dot{\boldsymbol{\eta}} + \sum_{i=1}^{n}\frac{k_{pi}}{2\epsilon_i} \\ &= -\dot{\boldsymbol{\eta}}^{\mathrm{T}}\left(\boldsymbol{E} - \sum_{i=1}^{n} e_{\epsilon i}\boldsymbol{R}_i^{\mathrm{T}}\boldsymbol{R}_i\right)\dot{\boldsymbol{\eta}} - \sum_{i=1}^{n} k_{di}\boldsymbol{\omega}_i^{\mathrm{T}}\boldsymbol{\omega}_i + \sum_{i=1}^{n}\frac{k_{pi}}{2\epsilon_i} \end{aligned} \tag{11}$$

where $e_{\epsilon i} = k_{pi}\boldsymbol{q}^2\epsilon_i/2$. We can always find n ϵ_i such that the matrix $(\boldsymbol{E} - \sum_{i=1}^{n} e_{\epsilon i}\boldsymbol{R}_i^{\mathrm{T}}\boldsymbol{R}_i)$ is positive definite. Thus, the system Eq.(1) and Eq.(3) is ultimately uniformly bounded with the control law Eq.(7). Obviously, when the disturbance $\boldsymbol{T}_d$ is bounded, following the above derivation can also prove that the system is ultimately uniformly bounded.

It can be seen that when k_{pi} and k_{di} are determined, attitude control and vibration suppression can be performed. Substituting Eq.(7) into the former equation of Eq.(2) yields

$$\boldsymbol{T}_c = -\sum_{i=1}^{n} k_{pi}\boldsymbol{q} - \sum_{i=1}^{n} k_{di}\boldsymbol{\omega} - \sum_{i=1}^{n}\left(k_{di}\dot{\boldsymbol{\beta}}_i\right) \tag{12}$$

With the above form, the actual meaning of each part of the control law can be roughly explained as follows: the first two parts are the proportional-derivative control law to stabilize the attitude motion of spacecraft, and the last part is the angular velocity damping used to attenuate the vibration at the mounting nodes of actuators. However, $\boldsymbol{T}_i$ acts on both the attitude dynamics Eq.(1a) and elastic dynamics Eq.(1b). How to design k_{pi} and k_{di} will be explained in section IV.

IV. Distributed Optimization Method

In this section, firstly, the attitude control and vibration suppression of flexible spacecraft is formulated as a distributed optimization problem about obtaining the parameters k_{pi} and k_{di}. Then, a method to deal with the output saturation of actuators is proposed. Thereafter a distributed optimization method based on surplus idea is elaborated. Finally, the convergence of the proposed method is analyzed.

A. Problem Formulation

In the discussion in the previous section, the constraints on control gains k_{pi} and k_{di} are only to be positive. To meet the specific dynamic and steady-state performance of spacecraft control, k_{pi} and k_{di} are required to satisfy the following equality constraints

$$\begin{cases} \sum_{i=1}^{n} k_{pi} = k_p; \\ \sum_{i=1}^{n} k_{di} = k_d. \end{cases} \tag{13}$$

where k_p and k_d are parameters designed according to specific missions. It can be seen that the Eq.(13) are global constraints on k_{pi} and k_{di}. Note that if the actuators use another kind of control law, there can be some global constraints on the parameters of that control law. We focus on considering how to deal with global equality constraints like these.

Besides, the output torques of the actuators should satisfy certain saturation constraints

$$\underline{\boldsymbol{u}}_i \preceq \boldsymbol{T}_i \preceq \overline{\boldsymbol{u}}_i,\ i = 1, \cdots, n. \tag{14}$$

where $\underline{\boldsymbol{u}}_i = [\underline{u}_{i1},\ \underline{u}_{i2},\ \underline{u}_{i3}]^{\mathrm{T}} \in \mathbb{R}^3$ and $\overline{\boldsymbol{u}}_i = [\overline{u}_{i1},\ \overline{u}_{i2},\ \overline{u}_{i3}]^{\mathrm{T}} \in \mathbb{R}^3$ represent the lower and upper bounds of the three-axis torque output at the actuator mounting node A_i, respectively. For any $\boldsymbol{a},\ \boldsymbol{b} \in \mathbb{R}^{m\times n}$, we say $\boldsymbol{a} \preceq \boldsymbol{b}$ if all the entries of

$\boldsymbol{a} - \boldsymbol{b}$ are nonpositive and $\boldsymbol{a} \geq \boldsymbol{b}$ if all the entries of $\boldsymbol{a} - \boldsymbol{b}$ are nonnegative. The inequality constraints in Eq.(14) are local since they contain only undetermined parameters at node A_i.

From the perspective of vibration suppression, it is desired to make $\sum_{i=1}^{n} \dot{\boldsymbol{\beta}}_i^{\mathrm{T}} \boldsymbol{T}_i$ as negative as possible, as this can provide as much damping as possible [17]. Nevertheless, since $\sum_{i=1}^{n} \dot{\boldsymbol{\beta}}_i^{\mathrm{T}} \boldsymbol{T}_i$ is a linear function with respect to k_{pi} and k_{di}, the optimal solution about it will be obtained at the boundary of the feasible set. When the attitude is in a small neighborhood of the stable point, it is not desirable for the torque $\boldsymbol{T}_i$ to take saturated values frequently. Therefore, a quadratic objective function for vibration suppression is proposed here. To obtain the quadratic form, considering control law Eq.(7) to expand $\sum_{i=1}^{n} \dot{\boldsymbol{\beta}}_i^{\mathrm{T}} \boldsymbol{T}_i$, we have

$$\sum_{i=1}^{n} \dot{\boldsymbol{\beta}}_i^{\mathrm{T}} \boldsymbol{T}_i = \sum_{i=1}^{n} \left[k_{pi}(-\dot{\boldsymbol{\beta}}_i^{\mathrm{T}} \boldsymbol{q}) + k_{di}(-\dot{\boldsymbol{\beta}}_i^{\mathrm{T}} \omega_i) \right] \tag{15}$$

where $-\dot{\boldsymbol{\beta}}_i^{\mathrm{T}} \boldsymbol{q}$ and $-\dot{\boldsymbol{\beta}}_i^{\mathrm{T}} \omega_i$ can be used to construct a weight matrix. To avoid the singularity in calculation process, a "sigmoid" operation is proposed to map $-\dot{\boldsymbol{\beta}}_i^{\mathrm{T}} \boldsymbol{q}$ and $-\dot{\boldsymbol{\beta}}_i^{\mathrm{T}} \omega_i$ into interval $(0, 1)$. Thus, the objective function for vibration suppression can be

$$J_s = \frac{1}{2} \sum_{i=1}^{n} \boldsymbol{k}_i^{\mathrm{T}} \boldsymbol{P}_i \boldsymbol{k}_i \tag{16}$$

where $\boldsymbol{k}_i = [k_{pi}, k_{di}]^{\mathrm{T}}$, and $\boldsymbol{P} = \mathrm{diag}(P_{i1}, P_{i2})$ with the following specific definition

$$\boldsymbol{P}_i = \begin{bmatrix} f(-\dot{\boldsymbol{\beta}}_i^{\mathrm{T}} \boldsymbol{q}) & 0 \\ 0 & f(-\dot{\boldsymbol{\beta}}_i^{\mathrm{T}} \omega_i) \end{bmatrix} \tag{17}$$

in which $f(\cdot)$ denotes a sigmoid function

$$f(x) = \frac{1}{1 + a \exp(-bx)} \tag{18}$$

with $a, b > 0$ are design parameters.

Obviously, minimizing Eq.(16) will obtain a different results from minimizing $\sum_{i=1}^{n} \dot{\boldsymbol{\beta}}_i^{\mathrm{T}} \boldsymbol{T}_i$. However, minimizing Eq.(16) also reduces $\sum_{i=1}^{n} \dot{\boldsymbol{\beta}}_i^{\mathrm{T}} \boldsymbol{T}_i$, which increases the damping of the system without frequently taking boundary values. In this sense, minimizing Eq.(16) enables vibration suppression. To realize the energy regulation, following term is considered

$$J_e = \frac{1}{2} \sum_{i=1}^{n} \boldsymbol{T}_i^{\mathrm{T}} \boldsymbol{S}_i \boldsymbol{T}_i \tag{19}$$

where $\boldsymbol{S}_i = \mathrm{diag}(S_{i1}, S_{i2}, S_{i3})$ are diagonal positive definite matrices to be designed.

So far, we can formulate the attitude control and vibration suppression of flexible spacecraft to a standard optimization problem as follows. To avoid confusing, these notations are used hereinafter: $x_{pi} \equiv k_{pi}$, $x_{di} \equiv k_{di}$, $x_p \equiv k_p$, $x_d \equiv$

k_d, $\boldsymbol{x}_i \equiv \boldsymbol{k}_i$.

$$\min \quad J(\boldsymbol{x}_1, \cdots, \boldsymbol{x}_n) = J_s + J_e = \frac{1}{2}\sum_{i=1}^{n} \boldsymbol{x}_i^{\mathrm{T}} \boldsymbol{P}_i \boldsymbol{x}_i + \frac{1}{2}\sum_{i=1}^{n} \boldsymbol{T}_i^{\mathrm{T}} \boldsymbol{S}_i \boldsymbol{T}_i$$
$$\text{s.t.} \quad \begin{cases} \underline{\boldsymbol{u}}_i \preceq -\boldsymbol{q} x_{pi} - \omega_i x_{di} \preceq \overline{\boldsymbol{u}}_i \\ 0 \leq x_{pi} \leq \overline{x}_{pi} \\ 0 \leq x_{di} \leq \overline{x}_{di} \\ \sum_{i=1}^{n} x_{pi} = x_p \\ \sum_{i=1}^{n} x_{di} = x_d \end{cases} \qquad i = 1, \cdots, n. \tag{20}$$

where $\overline{x}_{pi}$ and $\overline{x}_{di}$ are the upper bounds for x_{pi} and x_{di}. From Eq.(20), it can be seen that the performance of attitude control is formulated into the constraints, and the index of vibration suppression is arranged as the objective function of the optimization problem. This complies with the desire to keep vibration as small as possible while achieving attitude control goals.

B. Problem Solution

It is not easy to solve the problem Eq.(20) directly due to the coupling constraints between x_{pi} and x_{di} (saturation constraints). Therefore, consider introducing another local variable $\boldsymbol{y}_i = -x_{pi}\boldsymbol{q} - x_{di}\omega_i$ for node A_i and transform the problem Eq.(20) into the following equivalent problem

$$\min \quad \frac{1}{2}\sum_{i=1}^{n} \boldsymbol{x}_i^{\mathrm{T}} \boldsymbol{P}_i \boldsymbol{x}_i + \frac{1}{2}\sum_{i=1}^{n} \boldsymbol{y}_i^{\mathrm{T}} \boldsymbol{S}_i \boldsymbol{y}_i$$
$$\text{s.t.} \quad \begin{cases} \underline{\boldsymbol{u}}_i \preceq \boldsymbol{y}_i \preceq \overline{\boldsymbol{u}}_i \\ \boldsymbol{y}_i = -\boldsymbol{q} x_{pi} - \omega_i x_{di} \\ 0 \leq x_{pi} \leq \overline{x}_{pi} \\ 0 \leq x_{di} \leq \overline{x}_{di} \\ \sum_{i=1}^{n} x_{pi} = x_p \\ \sum_{i=1}^{n} x_{di} = x_d \end{cases} \qquad i = 1, \cdots, n. \tag{21}$$

It can be seen that the variable $\boldsymbol{y}_i$ and the torque generated at node A_i, $\boldsymbol{T}_i$ have the same form. However, with this form, solving x_{pi}, x_{di} and $\boldsymbol{y}_i$ becomes two relatively independent processes, as will be seen later. This is an effective way to handle the local coupling constraints. Note that the problem Eq.(21) is a convex optimization problem and satisfies the Slater condition, which guarantees zero duality gap and the existence of a dual optimal solution [22].

The Lagrangian function of the problem Eq.(21) can be written as

$$L = \sum_{i=1}^{n} L_i + \nu_{cp}\left(x_p - \sum_{i=1}^{n} x_{pi}\right) + \nu_{cd}\left(x_d - \sum_{i=1}^{n} x_{di}\right) \tag{22}$$

in which,

$$\begin{aligned} L_i =& \frac{1}{2}\sum_{i=1}^{n} \boldsymbol{x}_i^{\mathrm{T}} \boldsymbol{P}_i \boldsymbol{x}_i + \frac{1}{2}\boldsymbol{y}_i^{\mathrm{T}} \boldsymbol{S}_i \boldsymbol{y}_i + \boldsymbol{\lambda}_{yui}^{\mathrm{T}}(\boldsymbol{y}_i - \overline{\boldsymbol{u}}_i) + \boldsymbol{\lambda}_{yli}^{\mathrm{T}}(\underline{\boldsymbol{u}}_i - \boldsymbol{y}_i) + \lambda_{pui}(x_{pi} - \overline{x}_{pi}) \\ &+ \lambda_{pli}(-x_{pi}) + \lambda_{dui}(x_{pi} - \overline{x}_{di}) + \lambda_{dli}(-x_{di}) + \boldsymbol{\nu}_i^{\mathrm{T}}(-\boldsymbol{y}_i - \boldsymbol{q}x_{pi} - \boldsymbol{\omega}_i x_{di}) \end{aligned} \tag{23}$$

where $\boldsymbol{\lambda}_{yui} \geq \mathbf{0}, \boldsymbol{\lambda}_{yli} \geq \mathbf{0}, \lambda_{pui} \geq 0, \lambda_{dui} \geq 0, \lambda_{pli} \geq 0, \lambda_{dli} \geq 0, \boldsymbol{\nu}_i, \nu_{cp}$ and ν_{cd} are Lagrange multipliers of appropriate dimensions. According to the KKT optimal conditions, the globally optimal solution $\boldsymbol{y}_i^*$ and the optimal Lagrange multiplier $\boldsymbol{\nu}_i^*$ should satisfy

$$\begin{cases} S_{ij}y_{ij}^* \leq \nu_{ij}^* & \text{for} \quad y_{ij}^* = \overline{u}_{ij} \\ S_{ij}y_{ij}^* = \nu_{ij}^* & \text{for} \quad \underline{u}_{ij} < y_{ij}^* < \overline{u}_{ij} \\ S_{ij}y_{ij}^* \geq \nu_{ij}^* & \text{for} \quad y_{ij}^* = \underline{u}_{ij} \end{cases}, j = 1, 2, 3. \tag{24}$$

where $\boldsymbol{\nu}_i = [\nu_{i1}, \nu_{i2}, \nu_{i3}]^{\mathrm{T}}$. The above condition Eq.(24) can also be written in the following equivalent form

$$y_{ij}^* = \psi_{yi}(\nu_{ij}^*) = \begin{cases} \overline{u}_{ij} & \text{if} \quad \nu_{ij}^* > S_{ij}\overline{u}_{ij} \\ S_{ij}^{-1}\nu_{ij}^* & \text{if} \quad S_{ij}\underline{u}_{ij} \leq \nu_{ij}^* \leq S_{ij}\overline{u}_{ij} \\ \underline{u}_{ij} & \text{if} \quad \nu_{ij}^* < S_{ij}\underline{u}_{ij} \end{cases}, j = 1, 2, 3. \tag{25}$$

Similarly, the globally optimal solution x_{pi}^* and x_{di}^* and the optimal Lagrange multipliers $\boldsymbol{\nu}_i^*$, ν_{cp}^* and ν_{cd}^* should satisfy

$$x_{pi}^* = \psi_{pi}(\boldsymbol{\nu}_i^*, \nu_{cp}^*) = \begin{cases} \overline{x}_{pi} & \text{if} \quad \nu_{cp}^* + \boldsymbol{q}^{\mathrm{T}}\boldsymbol{\nu}_i^* > P_{i1}\overline{x}_{pi} \\ P_{i1}^{-1}(\nu_{cp}^* + \boldsymbol{q}^{\mathrm{T}}\boldsymbol{\nu}_i^*) & \text{if} \quad 0 \leq \nu_{cp}^* + \boldsymbol{q}^{\mathrm{T}}\boldsymbol{\nu}_i^* \leq P_{i1}\overline{x}_{pi} \\ 0 & \text{if} \quad \nu_{cp}^* + \boldsymbol{q}^{\mathrm{T}}\boldsymbol{\nu}_i^* < 0 \end{cases} \tag{26}$$

and

$$x_{di}^* = \psi_{di}(\boldsymbol{\nu}_i^*, \nu_{cd}^*) = \begin{cases} \overline{x}_{di} & \text{if} \quad \nu_{cd}^* + \boldsymbol{\omega}_i^{\mathrm{T}}\boldsymbol{\nu}_i^* > P_{i2}\overline{x}_{di} \\ P_{i2}^{-1}(\nu_{cd}^* + \boldsymbol{\omega}_i^{\mathrm{T}}\boldsymbol{\nu}_i^*) & \text{if} \quad 0 \leq \nu_{cd}^* + \boldsymbol{\omega}_i^{\mathrm{T}}\boldsymbol{\nu}_i^* \leq P_{i2}\overline{x}_{di} \\ 0 & \text{if} \quad \nu_{cd}^* + \boldsymbol{\omega}_i^{\mathrm{T}}\boldsymbol{\nu}_i^* < 0 \end{cases} \tag{27}$$

The process of solving the above KKT conditions can of course be completed in a central calculation unit, and then the solutions can be distributed to different actuators. But what we are interested in is how to implement this process in a distributed way. When considering the actuator mounting node A_i, if it can obtain the global Lagrange multipliers ν_{cp}^* and ν_{cd}^*, the globally optimal solution can be gained by solving a equation set. In the next subsection, the method of obtaining the global Lagrange multipliers ν_{cp}^* and ν_{cd}^* for every actuator mounting node A_i in a distributed way will be discussed in detail.

C. Distributed Optimization Method

Distributed here means that each actuator can only exchange data with its neighboring actuators, and the entire process does not require a central processor to participate. To describe the communication topology of the actuators, graph is an efficient tool. An undirected graph $\mathcal{G} = (\mathcal{V}, \mathcal{E})$ consists of a nonempty finite set $\mathcal{V} = \{1, 2, \cdots, n\}$ of elements called vertices and a finite set $\mathcal{E} \subseteq \mathcal{V} \times \mathcal{V}$ of pairs of vertices called edges. An edge denoted by $(i, j) \in \mathcal{E}$ means vertices i and j are connected directly with each other. In the problem we consider, all indices i of the actuator mounting node A_i constitute the vertex set $\mathcal{V}$ of the graph. The neighbors of the ith vertex is denoted by $\mathcal{N}_i = \{j \in \mathcal{V} | (i, j) \in \mathcal{E}\}$. Physically, the actuator mounting node A_i can only exchange data with the vertices in its neighbors. For the convenience of subsequent discussion, we assume that each vertex belongs to its neighbors, namely $(i, i) \in \mathcal{N}_i$. This is reasonable since it means that the vertex i can obtain its own state information. The degree of vertex i is defined as $d_i = |\mathcal{N}_i|$, where $|\cdot|$ denotes the cardinality of a set. It is obvious that $d_i \neq 0$ in a connected graph.

To obtain the global Lagrange multipliers ν_{cp}^* and ν_{cd}^*, our main idea is to let each node A_i have its own copy of the Lagrange multipliers, say $\boldsymbol{\sigma}_i = [\sigma_{pi}, \sigma_{di}]^{\mathrm{T}} \in \mathbb{R}^2$, and update $\boldsymbol{\sigma}_i$ in a distributed manner such that all $\boldsymbol{\sigma}_i$ reach consensus at $\boldsymbol{\nu}_c^* = [\nu_{cp}^*, \nu_{cd}^*]^{\mathrm{T}} \in \mathbb{R}^2$. At this time, for each node A_i, if $\boldsymbol{\nu}_c^*$ is replaced by $\boldsymbol{\sigma}_i$ to solve the equations Eq.(30), the equality constraints $\sum_{i=1}^{n} x_{pi} = x_p$ and $\sum_{i=1}^{n} x_{di} = x_d$ (Eq.(13)) may not be satisfied. To overcome this challenge, a surplus variable $\boldsymbol{s}_i = [s_{pi}, s_{di}]^{\mathrm{T}}$ is introduced for each node to temporarily store the bias. By a smart consensus algorithm the bias will vanish asymptotically.

At this point, we are ready to state the distributed optimization algorithm. The initialization conditions are

$$
\begin{aligned}
&\sum_{i=1}^{n} \boldsymbol{x}_i(0) + \sum_{i=1}^{n} \boldsymbol{s}_i(0) = [x_p, x_d]^{\mathrm{T}}, \ \boldsymbol{x}_i(0) \succ \mathbf{0} \\
&\boldsymbol{y}_i(0) = \boldsymbol{Q}_i \boldsymbol{x}_i(0), \ \underline{\boldsymbol{u}}_i \preceq \boldsymbol{y}_i \preceq \overline{\boldsymbol{u}}_i, \ \boldsymbol{\nu}_i(0) = \boldsymbol{S}_i \boldsymbol{y}_i(0) \\
&\boldsymbol{\sigma}_i(0) = \boldsymbol{P}_i \boldsymbol{x}_i(0) + \boldsymbol{Q}_i^{\mathrm{T}} \boldsymbol{\nu}_i(0), \ i = 1, \cdots, n
\end{aligned}
\tag{28}
$$

Then, for node A_i,

(1) Update $\boldsymbol{\sigma}_i$

$$\boldsymbol{\sigma}_i(k+1) = \sum_{j \in \mathcal{N}_i} b_{i,j}\boldsymbol{\sigma}_j(k) + \varrho \boldsymbol{s}_i(k) \tag{29}$$

(2) Solve the following equation set

$$\begin{cases} x_{pi}(k+1) = \psi_{pi}(\boldsymbol{\nu}_i(k+1), \sigma_{pi}(k+1)) \\ x_{di}(k+1) = \psi_{di}(\boldsymbol{\nu}_i(k+1), \sigma_{di}(k+1)) \\ y_{ij}(k+1) = \psi_{yi}(\nu_{ij}(k+1)), \ j \in 1,2,3 \\ \boldsymbol{Q}_i\boldsymbol{x}_i(k+1) = \boldsymbol{y}_i(k+1) \end{cases} \tag{30}$$

(3) Update surplus variable $\boldsymbol{s}_i$

$$\boldsymbol{s}_i(k+1) = \sum_{j \in \mathcal{N}_i} c_{i,j}\boldsymbol{s}_j(k) - (\boldsymbol{x}_i(k+1) - \boldsymbol{x}_i(k)) \tag{31}$$

where $\boldsymbol{Q}_i = [-\boldsymbol{q}, -\boldsymbol{\omega}_i]$ is a matrix associated with the attitude of spacecraft and the angular velocity at node A_i, which is a constant matrix in each control period. $k \geq 0$ denotes the number of iterations. ϱ is a sufficiently small positive constant. $b_{i,j}$ and $c_{i,j}$ are defined as follows:

$$b_{i,j} = \begin{cases} \frac{1}{d_i} & \text{if } j \in \mathcal{N}_i \\ 0 & \text{otherwise} \end{cases}, \forall i, j \in \mathcal{V} \tag{32}$$

and

$$c_{i,j} = \begin{cases} \frac{1}{d_j} & \text{if } i \in \mathcal{N}_j \\ 0 & \text{otherwise} \end{cases}, \forall i, j \in \mathcal{V} \tag{33}$$

Eq.(30) is a eight-dimensional equation group that contains eight unknowns. It is not easy to solve it directly due to the nonlinearity involved. Motivated by the idea from [22], the Eq.(30) can be solved by gradient method as follows

$$\boldsymbol{\nu}_i^{(r+1)}(k+1) = \boldsymbol{\nu}_i^{(r)}(k+1) + \alpha_i\left[-\boldsymbol{y}_i^{(r)}(k+1) + \boldsymbol{Q}_i\boldsymbol{x}_i^{(r)}(k+1)\right] \tag{34a}$$

$$y_{ij}^{(r+1)}(k+1) = \psi_{yi}(\nu_{ij}^{(r+1)}(k+1)), \ j \in 1,2,3 \tag{34b}$$

$$x_{pi}^{(r+1)}(k+1) = \psi_{pi}(\boldsymbol{\nu}_i^{(r+1)}(k+1), \sigma_{pi}(k+1)) \tag{34c}$$

$$x_{di}^{(r+1)}(k+1) = \psi_{di}(\boldsymbol{\nu}_i^{(r+1)}(k+1), \sigma_{di}(k+1)) \tag{34d}$$

where $\alpha_i > 0$ is a constant stepsize of the gradient method; $r > 0$ is the number of iterations of the gradient method.

The implementation process of the proposed distributed optimization algorithm is shown in Fig.2. When all $\boldsymbol{\sigma}_i(k)$ reach to $\boldsymbol{v}_c^*$ and all $\boldsymbol{s}_i(k)$ converge to $\mathbf{0}$, the proposed algorithm will solve the KKT conditions of the problem Eq.(21) in a distributed way, which means all actuator mounting nodes will gain the globally optimal solution. The convergence of the algorithm will be analyzed in the next subsection.

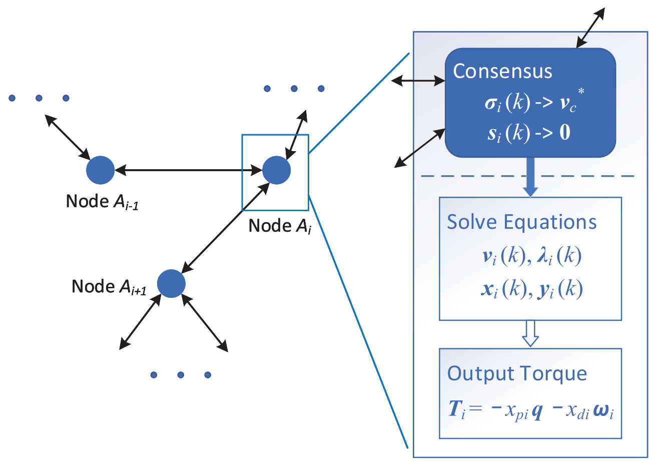

Fig. 2 Schematic of the proposed distributed optimization algorithm.

D. Convergence Analysis

In this subsection, the convergence analysis of the proposed algorithm is divided into two steps: first, analyze the case where neither $\boldsymbol{x}_i$ nor $\boldsymbol{y}_i$ is saturated; then the above method is extended to the case where the saturation constraints are considered.

If $\boldsymbol{x}_i$ and $\boldsymbol{y}_i$ are not saturated, referring to Eqs.(25)–(27) and $\boldsymbol{y}_i = \boldsymbol{Q}_i\boldsymbol{x}_i$, $\boldsymbol{v}_i$ can be derived as

$$\boldsymbol{v}_i = (\boldsymbol{S}_i^{-1} + \boldsymbol{Q}_i\boldsymbol{P}_i^{-1}\boldsymbol{Q}_i^{\mathrm{T}})^{-1}\boldsymbol{Q}_i\boldsymbol{P}_i^{-1}\boldsymbol{\sigma}_i \tag{35}$$

Then,

$$\boldsymbol{x}_i = \boldsymbol{Q}_{pi}\boldsymbol{\sigma}_i \tag{36}$$

where $\boldsymbol{Q}_{pi} = \boldsymbol{P}_i^{-1} - \boldsymbol{P}_i^{-1}\boldsymbol{Q}_i^{\mathrm{T}}(\boldsymbol{S}_i^{-1} + \boldsymbol{Q}_i\boldsymbol{P}_i^{-1}\boldsymbol{Q}_i^{\mathrm{T}})^{-1}\boldsymbol{Q}_i\boldsymbol{P}_i^{\mathrm{T}} \in \mathbb{R}^{2\times 2}$. The algorithm Eqs.(29)-(31) can be rewritten as

$$\boldsymbol{\sigma}(k+1) = \overline{\boldsymbol{B}}\boldsymbol{\sigma}(k) + \varrho\boldsymbol{s}(k) \tag{37a}$$

$$\boldsymbol{x}(k+1) = \boldsymbol{Q}_p\boldsymbol{\sigma}(k+1) \tag{37b}$$

$$\boldsymbol{s}(k+1) = \overline{\boldsymbol{C}}\boldsymbol{s}(k) - (\boldsymbol{x}(k+1) - \boldsymbol{x}(k)) \tag{37c}$$

where $\boldsymbol{Q}_p = \mathrm{diag}(\boldsymbol{Q}_{p1}, \cdots, \boldsymbol{Q}_{pn}) \in \mathbb{R}^{2n\times 2n}$, $\boldsymbol{\sigma} = [\boldsymbol{\sigma}_1^{\mathrm{T}}, \cdots, \boldsymbol{\sigma}_n^{\mathrm{T}}]^{\mathrm{T}}$, $\boldsymbol{s} = [\boldsymbol{s}_1^{\mathrm{T}}, \cdots, \boldsymbol{s}_n^{\mathrm{T}}]^{\mathrm{T}}$, $\boldsymbol{x}(k) = [\boldsymbol{x}_1^{\mathrm{T}}, \cdots, \boldsymbol{x}_n^{\mathrm{T}}]^{\mathrm{T}}$. $\overline{\boldsymbol{B}} = \boldsymbol{B} \otimes \boldsymbol{I}_2$ and $\overline{\boldsymbol{C}} = \boldsymbol{C} \otimes \boldsymbol{I}_2$ where the entries of $\boldsymbol{B}$ and $\boldsymbol{C}$ are defined by Eqs.(32) and (33), respectively. $\otimes$ denotes Kronecker product about two matrices. From the definition of $\boldsymbol{B}$ and $\boldsymbol{C}$, it is not difficult to verify that $\boldsymbol{B}$ is row stochastic, and $\boldsymbol{C}$ is column stochastic. That is, $\boldsymbol{B}\mathbf{1}_{2n} = \mathbf{1}_{2n}$ and $\mathbf{1}_{2n}^{\mathrm{T}}\boldsymbol{C} = \mathbf{1}_{2n}^{\mathrm{T}}$, where $\mathbf{1}_{2n} \in \mathbb{R}^{2n}$ is a column vector with all its entries being 1. Thereafter, Eq.(37c) preserves the summation of $\sum_{i=1}^{n} x_{pi}(k) + \sum_{i=1}^{n} s_{pi}(k)$ and $\sum_{i=1}^{n} x_{di}(k) + \sum_{i=1}^{n} s_{di}(k)$ over $\mathcal{V}$. Premultiplying both sides of Eq.(37c) by $(\mathbf{1}_n^{\mathrm{T}} \otimes [1,0]^{\mathrm{T}})$ we can obtain

$$
\begin{aligned}
(\mathbf{1}_n^{\mathrm{T}} \otimes [1,0]^{\mathrm{T}})\boldsymbol{s}(k+1) &= (\mathbf{1}_n^{\mathrm{T}} \otimes [1,0]^{\mathrm{T}})\overline{\boldsymbol{C}}\boldsymbol{s}(k) - (\mathbf{1}_n^{\mathrm{T}} \otimes [1,0]^{\mathrm{T}})\left(\boldsymbol{x}(k+1) - \boldsymbol{x}(k)\right) \\
&= (\mathbf{1}_n^{\mathrm{T}} \otimes [1,0]^{\mathrm{T}})\boldsymbol{s}(k) - (\mathbf{1}_n^{\mathrm{T}} \otimes [1,0]^{\mathrm{T}})\left(\boldsymbol{x}(k+1) - \boldsymbol{x}(k)\right)
\end{aligned}
\tag{38}
$$

that is,

$$
\sum_{i=1}^{n} x_{pi}(k+1) + \sum_{i=1}^{n} s_{pi}(k+1) = \sum_{i=1}^{n} x_{pi}(k) + \sum_{i=1}^{n} s_{pi}(k) \tag{39}
$$

Similarly, we can get $\sum_{i=1}^{n} x_{di}(k+1) + \sum_{i=1}^{n} s_{di}(k+1) = \sum_{i=1}^{n} x_{di}(k) + \sum_{i=1}^{n} s_{di}(k)$ by premultiplying both sides of Eq.(37c) by $\mathbf{1}_n^{\mathrm{T}} \otimes [0,1]^{\mathrm{T}}$. Recalling the initialization of $\boldsymbol{x}_i(0)$ and $\boldsymbol{s}_i(0)$, it is obvious that $\sum_{i=1}^{n} x_{pi}(k) + \sum_{i=1}^{n} s_{pi}(k) = x_p$, $\sum_{i=1}^{n} x_{di}(k) + \sum_{i=1}^{n} s_{di}(k) = x_d$, $\forall k > 0$.

Replacing $\boldsymbol{x}$ in Eq.(37c) with $\boldsymbol{\sigma}$ by using Eqs.(37a) and (37b) yields

$$
\boldsymbol{s}(k+1) = \boldsymbol{Q}_p(\boldsymbol{I}_{2n} - \overline{\boldsymbol{B}})\boldsymbol{\sigma}(k) + [\overline{\boldsymbol{C}} - \varrho\boldsymbol{Q}_p]\boldsymbol{s}(k) \tag{40}
$$

where $\boldsymbol{I}_{2n}$ is the $2n$-order identity matrix. Writing Eqs.(37a) and (40) in matrix form, we get

$$
\begin{bmatrix} \boldsymbol{\sigma}(k+1) \\ \boldsymbol{s}(k+1) \end{bmatrix} = \begin{bmatrix} \overline{\boldsymbol{B}} & \varrho\boldsymbol{I}_{2n} \\ \boldsymbol{Q}_p(\boldsymbol{I}_{2n} - \overline{\boldsymbol{B}}) & \overline{\boldsymbol{C}} - \varrho\boldsymbol{Q}_p \end{bmatrix} \begin{bmatrix} \boldsymbol{\sigma}(k) \\ \boldsymbol{s}(k) \end{bmatrix} \tag{41}
$$

Define

$$
\boldsymbol{\Gamma} = \begin{bmatrix} \overline{\boldsymbol{B}} & \mathbf{0} \\ \boldsymbol{Q}_p(\boldsymbol{I}_{2n} - \overline{\boldsymbol{B}}) & \overline{\boldsymbol{C}} \end{bmatrix}, \ \boldsymbol{\Delta} = \begin{bmatrix} \mathbf{0} & \boldsymbol{I}_{2n} \\ \mathbf{0} & -\boldsymbol{Q}_p \end{bmatrix}. \tag{42}
$$

The system matrix of Eq.(41) can be regarded as $\boldsymbol{\Gamma}$ perturbed by $\varrho\boldsymbol{\Delta}$. Since $\boldsymbol{\Gamma}$ is a lower block triangular matrix, the eigenvalues of $\boldsymbol{\Gamma}$ is the union of the eigenvalues of $\overline{\boldsymbol{B}}$ and $\overline{\boldsymbol{C}}$. According to the eigenvalue properties of Kronecker product and the definitions of $\overline{\boldsymbol{B}}$ and $\overline{\boldsymbol{C}}$, each eigenvalue of $\boldsymbol{B}$ corresponds to two identical eigenvalues of $\overline{\boldsymbol{B}}$, as do of $\boldsymbol{C}$ and $\overline{\boldsymbol{C}}$. Thus, $\boldsymbol{\Gamma}$ has four eigenvalues $\gamma_i = 1,\ i = 1,2,3,4$, and the rest eigenvalues lie in the open unit disk on the complex plane. Next, the matrix perturbation theory is applied to analyze the behavior of γ_i under perturbation $\varrho\boldsymbol{\Delta}$.

Construct eigenvector sets $\boldsymbol{U}$ and $\boldsymbol{V}^{\mathrm{T}}$ as follows

$$\boldsymbol{U} = \begin{bmatrix} \mathbf{0} & \boldsymbol{\phi}_1 \\ \boldsymbol{\phi}_2 & -\boldsymbol{\phi}_2\boldsymbol{\varphi}_2^{\mathrm{T}}\boldsymbol{Q}\boldsymbol{\phi}_1 \end{bmatrix},\ \boldsymbol{V}^{\mathrm{T}} = \begin{bmatrix} \boldsymbol{\varphi}_2^{\mathrm{T}}\boldsymbol{Q} & \boldsymbol{\varphi}_2^{\mathrm{T}} \\ \boldsymbol{\varphi}_1^{\mathrm{T}} & \mathbf{0}^{\mathrm{T}} \end{bmatrix}. \tag{43}$$

where

$$\boldsymbol{\phi}_1 = \mathbf{1}_n \otimes \boldsymbol{I}_2,\ \boldsymbol{\varphi}_1^{\mathrm{T}} = \boldsymbol{\varpi}^{\mathrm{T}} \otimes \boldsymbol{I}_2 \tag{44}$$

are linearly independent right and left eigenvectors corresponding to the two unit eigenvalues of $\overline{\boldsymbol{B}}$, in which, $\boldsymbol{\varpi} \in \mathbb{R}^n$ satisfies $\mathbf{1}_n^{\mathrm{T}}\boldsymbol{\varpi} = 1$ and $\boldsymbol{\varpi} \geq \mathbf{0}$.

$$\boldsymbol{\phi}_2 = \boldsymbol{\mu} \otimes \boldsymbol{I}_2,\ \boldsymbol{\varphi}_2^{\mathrm{T}} = \mathbf{1}_n^{\mathrm{T}} \otimes \boldsymbol{I}_2 \tag{45}$$

are linearly independent right and left eigenvectors corresponding to the two unit eigenvalues of $\overline{\boldsymbol{C}}$, in which, $\boldsymbol{\mu} \in \mathbb{R}^n$ satisfies $\mathbf{1}_n^{\mathrm{T}}\boldsymbol{\mu} = 1$ and $\boldsymbol{\mu} \geq \mathbf{0}$.

It can be proved that $\boldsymbol{U}$ and $\boldsymbol{V}^{\mathrm{T}}$ are the four linearly independent right and left eigenvectors of $\boldsymbol{\Gamma}$ corresponding to the eigenvalues γ_i. Furthermore, $\boldsymbol{V}^{\mathrm{T}}\boldsymbol{U} = \boldsymbol{I}_{4n}$. If ϱ is small, the variation of γ_i perturbed by $\varrho\boldsymbol{\Delta}$ can be quantified by the eigenvalues of $\boldsymbol{V}^{\mathrm{T}}\boldsymbol{\Delta}\boldsymbol{U}$. Since

$$\boldsymbol{V}^{\mathrm{T}}\boldsymbol{\Delta}\boldsymbol{U} = \begin{bmatrix} \mathbf{0} & \mathbf{0} \\ (\boldsymbol{\varpi}^{\mathrm{T}}\boldsymbol{\mu})\boldsymbol{I}_2 & -\boldsymbol{\varphi}_1^{\mathrm{T}}\boldsymbol{\phi}_2\boldsymbol{\varphi}_2^{\mathrm{T}}\boldsymbol{Q}\boldsymbol{\phi}_1 \end{bmatrix} \tag{46}$$

two of the eigenvalues of $\boldsymbol{V}^{\mathrm{T}}\boldsymbol{\Delta}\boldsymbol{U}$ are 0. Thus, $(\mathrm{d}\gamma_1)/(\mathrm{d}\varrho) = (\mathrm{d}\gamma_2)/(\mathrm{d}\varrho) = 0$, which means γ_1 and γ_2 do not change against ϱ. Recalling the definition of $\boldsymbol{Q}$ and Eqs.(44) and (45), we have

$$\begin{aligned} & -\boldsymbol{\varphi}_1^{\mathrm{T}}\boldsymbol{\phi}_2\boldsymbol{\varphi}_2^{\mathrm{T}}\boldsymbol{Q}\boldsymbol{\phi}_1 = -(\boldsymbol{\varpi}^{\mathrm{T}}\boldsymbol{\mu}\mathbf{1}_n^{\mathrm{T}} \otimes \boldsymbol{I}_2)\boldsymbol{Q}(\mathbf{1}_n^{\mathrm{T}} \otimes \boldsymbol{I}_2) \\ =& -\boldsymbol{\varpi}^{\mathrm{T}}\boldsymbol{\mu}\,[\boldsymbol{I}_2, \cdots, \boldsymbol{I}_2]\,\mathrm{diag}(\boldsymbol{Q}_{p1}, \cdots, \boldsymbol{Q}_{pn})\,[\boldsymbol{I}_2, \cdots, \boldsymbol{I}_2]^{\mathrm{T}} \\ =& -\boldsymbol{\varpi}^{\mathrm{T}}\boldsymbol{\mu}\sum_{i=1}^{n}\boldsymbol{Q}_{pi} \end{aligned} \tag{47}$$

It can be verified that all leading principal minors of the matrix $\sum_{i=1}^{n}\boldsymbol{Q}_{pi}$ are positive. Thus, all the eigenvalues of $\sum_{i=1}^{n}\boldsymbol{Q}_{pi}$ are positive, which results in $(\mathrm{d}\gamma_3)/(\mathrm{d}\varrho) < 0$ and $(\mathrm{d}\gamma_4)/(\mathrm{d}\varrho) < 0$. If $\varrho > 0$, γ_3 and γ_4 become smaller. Let $\overline{\varrho}_1$ be the upper bound of ϱ such that when $\varrho < \overline{\varrho}_1$, $|\gamma_3| < 1$ and $|\gamma_4| < 1$. In addition, since eigenvalues are continuous function of matrix entries, there must exist an upper bound $\overline{\varrho}_2$ such that when $\varrho < \overline{\varrho}_2$, the rest eigenvalues of $(\boldsymbol{\Gamma} + \varrho\boldsymbol{\Delta})$, $|\gamma_i| < 1,\ i = 5, 6, \cdots, 4n$. Thus for any sufficiently small $\varrho \in (0, \min\{\overline{\varrho}_1, \overline{\varrho}_2\})$, the spectral radius of $\boldsymbol{\Gamma} + \varrho\boldsymbol{\Delta}$, $\rho(\boldsymbol{\Gamma} + \varrho\boldsymbol{\Delta}) = 1$ and $|\gamma_i| < 1,\ i = 3, 4, \cdots, 4n$.

Since $[(\mathbf{1}_n \otimes \boldsymbol{I}_2)^{\mathrm{T}}, \mathbf{0}^{\mathrm{T}}]^{\mathrm{T}}$ is the eigenvectors associated with $\gamma_1 = \gamma_2 = 1$ of the system matrix $(\boldsymbol{\Gamma} + \varrho\boldsymbol{\Delta})$ in Eq.(41)

and all its rest eigenvalues are within the open unit disk, thus

$$\lim_{k\to\infty}\begin{bmatrix}\boldsymbol{\sigma}(k)\\ \boldsymbol{s}(k)\end{bmatrix}=\text{span}\begin{bmatrix}\mathbf{1}_n\otimes\boldsymbol{I}_2\\ \mathbf{0}\end{bmatrix} \tag{48}$$

That is, $s_{pi}\to 0$, $s_{di}\to 0$ as $k\to\infty$, $\forall i$. Referring to Eq.(39), it can be derived that $\sum_{i=1}^{n}x_{pi}(k)=x_p$ and $\sum_{i=1}^{n}x_{di}(k)=x_d$ as $k\to\infty$, $\forall i$. The equality constraints Eq.(13) are satisfied. From the upper half of Eq.(48), $\sigma_{pi}(k)$ and $\sigma_{di}(k)$ will converge to two same values, respectively. According to the discussion in the previous subsection, we have $\sigma_{pi}(k)\to\nu_{cp}^{*}$ and $\sigma_{di}(k)\to\nu_{cd}^{*}$ as $k\to\infty$, $\forall i$.

At this point, the convergence of the proposed algorithm has been demonstrated without considering saturation constraints. Next, we consider the case of torque saturation, that is, some $\boldsymbol{y}_i$ are saturated regardless of whether $\boldsymbol{x}_i$ are saturated.

It can be seen from the above analysis that the algorithm Eq.(37) is a feedback system with ϱ as the gain. By premultiplying $(\mathbf{1}_n^{\mathrm{T}}\otimes[1,0]^{\mathrm{T}})$ from both sides of Eq.(37a), it can be obtained that

$$\sum_i\sigma_{pi}(k+1)=\sum_{i,j}b_{i,j}\sigma_{pj}(k)+\varrho e_p(k) \tag{49}$$

where $e_p(k)=x_p-\sum_{i=1}^{n}\sigma_{pi}(k)$ (recall Eq.(39)) is the gap between the actual parameters and the target parameter regarding the equality constraints of attitude control. Without loss of generality, assume $e_p(k)>0$, then the overall level of $\sigma_{pi}(k)$ will increase and each $\sigma_{pi}(k)$ will approach to the same value ν_{cp}^{*}. And according to Eq.(37b), $x_{pi}(k+1)$ is an increasing function with respect to $\sigma_{pi}(k+1)$, which leads to $\sum_{i=1}^{n}x_{pi}(k+1)-\sum_{i=1}^{n}x_{pi}(k)>0$. Then, we have $e_p(k+1)<e_p(k)$ from Eq.(37c). The feedback in Eq.(37) will reduce the gap $e_p(k)$. Similarly, there also exists a feedback between $\sum_i\sigma_{di}(k)$ and $e_d(k)=x_d-\sum_{i=1}^{n}\sigma_{di}(k)$. In this process, some of the actuators may reach the torque saturation. After an iteration $\underline{k}$, if actuator node A_i is saturated, then for $k>\underline{k}$, node A_i will hold saturation. Considering the actuator saturation, the algorithm Eq.(41) can be revised as

$$\begin{bmatrix}\boldsymbol{\sigma}(k+1)\\ \boldsymbol{s}(k+1)\end{bmatrix}=\begin{bmatrix}\overline{\boldsymbol{B}} & \varrho\boldsymbol{I}_{2n}\\ \overline{\boldsymbol{Q}}_p(\boldsymbol{I}_{2n}-\overline{\boldsymbol{B}}) & \overline{\boldsymbol{C}}-\varrho\overline{\boldsymbol{Q}}_p\end{bmatrix}\begin{bmatrix}\boldsymbol{\sigma}(k)\\ \boldsymbol{s}(k)\end{bmatrix} \tag{50}$$

where $\overline{\boldsymbol{Q}}_p=\text{diag}(\overline{\boldsymbol{Q}}_{p1},\cdots,\overline{\boldsymbol{Q}}_{pn})\in\mathbb{R}^{2n\times 2n}$, in which

$$\overline{\boldsymbol{Q}}_{pi}=\begin{cases}\mathbf{0} & \text{if actuator node } A_i \text{ is saturated}\\ \boldsymbol{Q}_{pi} & \text{otherwise}\end{cases} \tag{51}$$

Following the similar eigenvalue perturbation analysis, the above system Eq.(50) can be proven to be stable. The last case, where some $\boldsymbol{x}_i$ are saturated and $\boldsymbol{y}_i$ is not, can be analyzed by following the procedure of Eqs.(49)-(51). Obviously the proposed method is still convergent in this case. Hence, the proposed algorithm will solve the KKT conditions of the problem Eq.(21) in a distributed way, and all actuator nodes will get the globally optimal solution.

Remark 1 When the gradient method Eq.(34) is used to solve the local equations Eq.(30), if an adaptive diminishing stepsize $\alpha_i(r)$ that varies with each iteration is adopted, the Eq.(34) can converge to the optimal solution as $r \to \infty$. If a constant stepsize α_i is adopted, the Eq.(34) will converge to an interval containing the optimal solution, where the error bound is related to the stepsize α_i and iteration number r [22]. Smaller stepsize and more iterations will result in smaller error bounds. If the stepsize α_i is small sufficient, the iteration error with respect to $\boldsymbol{x}_i^{(r)}(k)$ can be lumped into the matrix $\boldsymbol{Q}_i$ for analysis.

Remark 2 For the selection of parameter ϱ, one can refer to [23], which gives a conservative bound on ϱ. An optimized ϱ can also be obtained by an optimization method.

V. Numerical simulation

The proposed distributed optimization algorithm is applied to an unconstrained flexible spacecraft in this section to demonstrate its effectiveness. The considered spacecraft is a uniform elastic plate sizing 6m × 10m. 8 sets of three-axis orthogonal reaction-wheel systems are installed at the actuator mounting nodes $A_i(i = 1, \cdots, 8)$ for attitude control and vibration suppression. The communication topology and mounting positions of the actuator nodes is shown in Fig.3. The circles marked numbers denote actuator mounting nodes; the lines represent the interactions between actuator nodes. By the finite element method, the inertia matrix of the system is diag$(2251.6, 5940.5, 8189.3)$ (kg·m^2), and the fundamental frequency of the whole system is 0.8424 Hz. Six unconstrained modes are selected by the inertia completeness criteria in the simulation of dynamics. The other five mode frequencies selected are 1.9644 Hz, 2.3066 Hz, 2.9550 Hz, 3.5186 Hz, and 4.2664 Hz. The damping coefficients of the selected modes are assumed to be constants $\xi_i = 0.005, i = 1, \cdots, 6$.

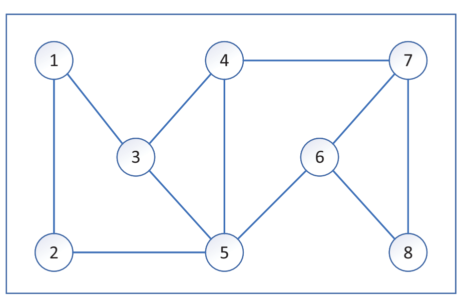

Fig. 3 Communication topology of actuator nodes.

To fully verify the effectiveness of the proposed method, a sequence of large-angle attitude maneuvers are implemented in the simulation. There are two 165° attitude maneuver commands at 190s and 320s, respectively, and the Euler axis is assumed to be $[0.8729, -0.4364, 0.2182]^{\mathrm{T}}$. Referring to [14, 17], the initial parameters of the system are assumed to be

$$[q_0(0), \boldsymbol{q}^{\mathrm{T}}(0)]^{\mathrm{T}} = [-0.4386, -0.4821, -0.5576, 0.5140]^{\mathrm{T}}$$

$$\boldsymbol{\omega}(0) = [3 \times 10^{-4}, 5 \times 10^{-3}, 1 \times 10^{-4}]^{\mathrm{T}} \text{ rad/s}$$

$$\boldsymbol{\eta}(0) = [5.6311, 4.0732, 3.7053, -0.4255, -0.8020, 0.7464] \times 10^{-3}$$

$$\dot{\boldsymbol{\eta}}(0) = [3.3687, 0.6147, -3.0043, -2.2010, 0.1501, -0.1176] \times 10^{-4}$$

Two cases are considered in the simulation. In case I, the distributed vibration suppression method based on control allocation [17] is adopted. In case II, the control law Eq.(7) is adopted and the proposed distributed optimization algorithm is utilized to obtain the control gains. In both cases, the maximum output torque of the actuator is considered to be 2 Nm, and the control period is set to be 0.08 s. Some parameters of case II are set as follows: the constraints on the control gains are assumed to be $\sum_{i=1}^{n} x_{pi} = x_p = 40$ and $\sum_{i=1}^{n} x_{di} = x_d = 500$. The initializations are chosen as $x_{pi}(0) = 40/8$, $x_{di}(0) = 500/8$, $i = 1, \cdots, 8$. The parameters in the algorithm are chosen as follows: $\varrho = 0.006$ in Eq.(29); The gradient method Eq.(34) is adopted to solve the equations Eq.(30) and α_i is chosen as 0.008. The number of iterations of the proposed algorithm is set to be 8. Since the difference of initial values between the two adjacent control cycles are not distinct, a small number of iterations is chosen. In addition, there are almost only elementary mathematical operations in the proposed algorithm, thus its execution is fast.

The simulation results are shown in Figs.4~9. The time histories of the Euler angles and angular velocity errors are similar in the two cases. For the sake of brevity, only those of the case II are shown in Figs.4(a) and 4(b).

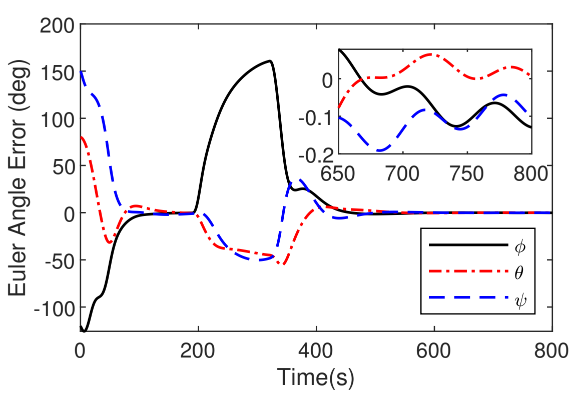

(a) Euler angles.

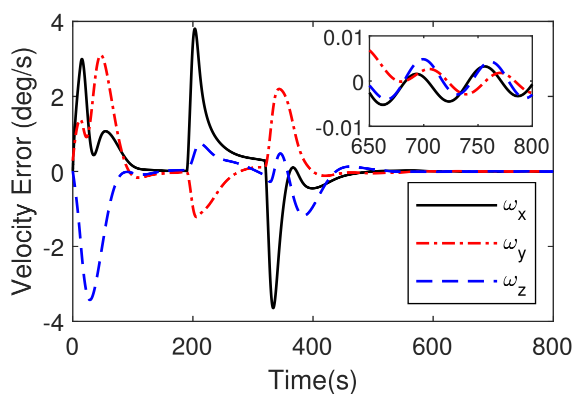

(b) Angular velocities.

Fig. 4 Spacecraft Attitude.

Fig.5 shows the time history of the modal coordinates. It can be found that, by the proposed distributed optimization

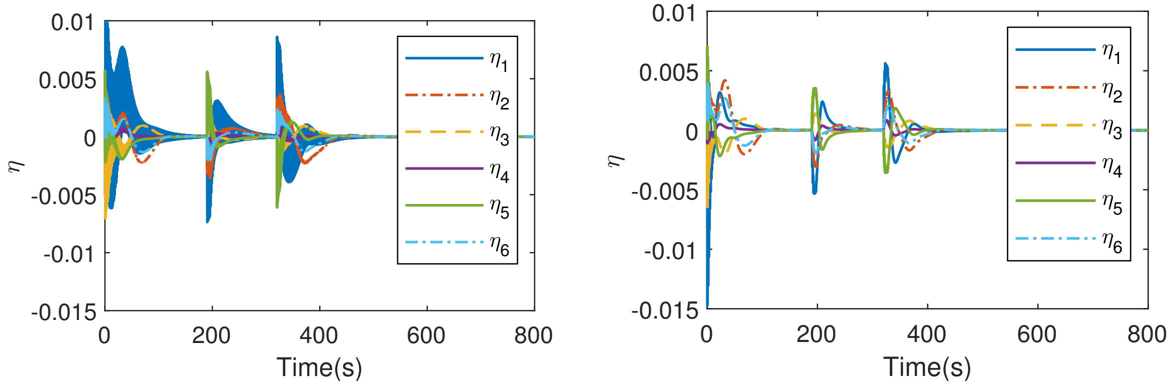

(a) Case I (b) Case II

Fig. 5 Modal coordinates.

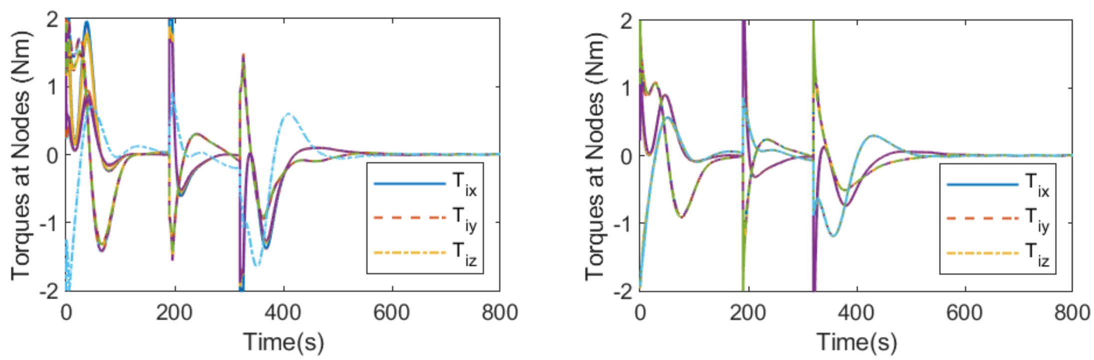

(a) Case I (b) Case II

Fig. 6 Torques of actuators.

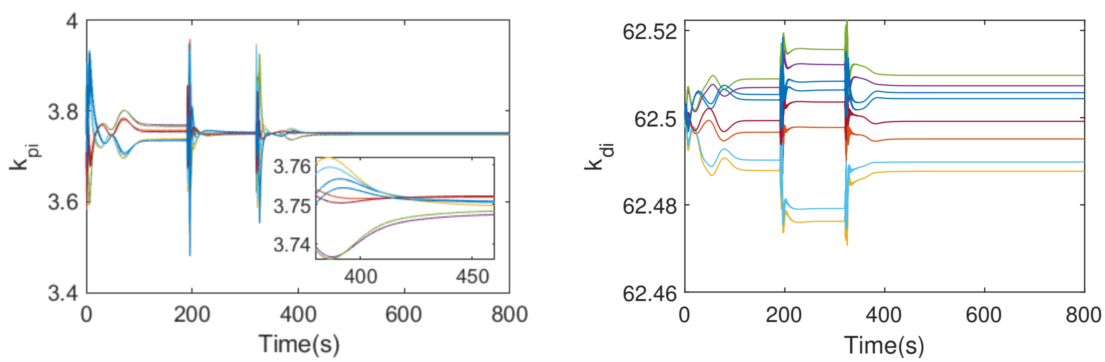

(a) $\boldsymbol{k}_{pi}$ (b) $\boldsymbol{k}_{di}$

Fig. 7 Optimal control gains k_{pi} and k_{di}.

algorithm, the vibration of the system is not as severe as that of the distributed control allocation method [17]. The reason is that the method in [17] does not consider the torque saturation of the actuators and it also requires a high control frequency to achieve superior control performance. This is a limitation of the method itself, independent of the

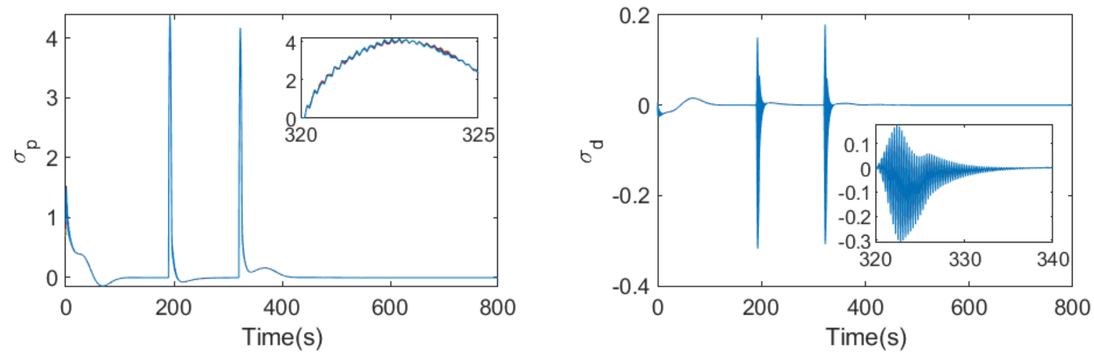

(a) σ_{pi} (b) σ_{di}

Fig. 8 Consensus variables σ.

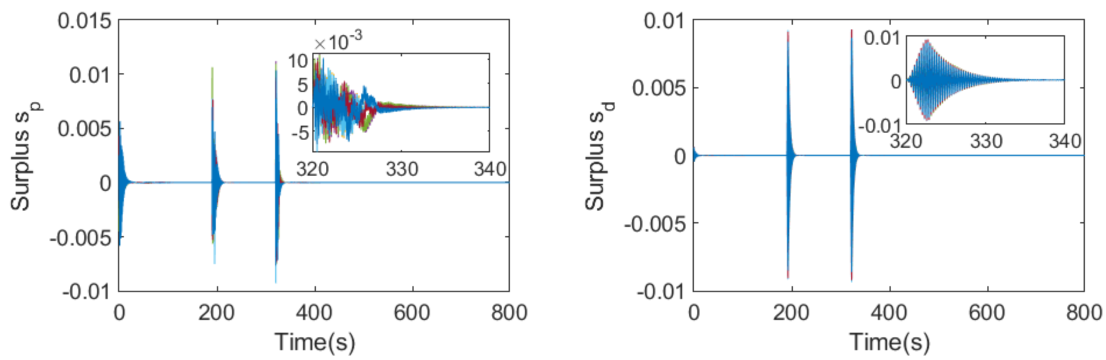

(a) s_{pi} (b) s_{di}

Fig. 9 Surplus variables s.

choice of the control law parameters. The time histories of the torques generated at all the 8 actuator mounting nodes are shown in Fig.6. In Fig.6, different line types represent different torque output axes, and different colors represent different actuator mounting nodes. The time histories of the control gains by the proposed distributed optimization algorithm are show in Fig.7. The differences of the control gains at different nodes are not large, the reason is that the difference of the vibration state matrices $\boldsymbol{P}_i$ of each nodes are not large. By increasing the difference of the vibration state matrices $\boldsymbol{P}_i$, the difference of the control gains among the nodes can be increased, so as to better suppress the vibration. But this will also increase the torque saturation possibility of actuator nodes. The consensus variable $\boldsymbol{\sigma}$ and the surplus variable $\boldsymbol{s}$ are shown in Fig.8 and Fig.9, respectively. It can be seen that the convergence speed of the algorithm is relatively fast. At the same time, it can be verified that the equality constraints on the control gains are satisfied when the algorithm converges.

Compared with the method in [17], the method in this paper does not require a centralized control unit to generate the control torque. The implementation of the proposed method here is in a more thoroughly distributed way. Meanwhile, the method in this paper has a certain energy regulation ability due to the introduction of the term J_e in objective function.

VI. Conclusion

A distributed optimization method is proposed to handle the attitude control and vibration suppression of flexible spacecraft. The momentum exchange actuators are scattered across the spacecraft. By assuming each actuator mounting node adopts the same form of control law, after determining the control gains of each nodes the attitude control and vibration suppression can be realized in a thoroughly distributed way. The centralized control unit is not required. The stability of the control law is analyzed by the Lyapunov method. The dynamic and steady-state performance of the attitude control is formulated into equality constraints. The vibration of the system is formulated as the objective function of the optimization problem. A surplus based consensus method is proposed to solve the KKT conditions of the optimization problem in a distributed way. Numerical simulations demonstrate the effectiveness of the proposed algorithm. Compared with the distributed vibration suppression method based on control allocation, the proposed method has a better performance and does not require high control frequency.

References

[1] Singhose, W. E., Banerjee, A. K., and Seering, W. P., "Slewing flexible spacecraft with deflection-limiting input shaping," *Journal of Guidance, Control, and Dynamics*, Vol. 20, No. 2, 1997, pp. 291–298. doi:10.2514/2.4036.

[2] Fracchia, G., Biggs, J. D., and Ceriotti, M., "Analytical low-jerk reorientation maneuvers for multi-body spacecraft structures," *Acta Astronautica*, Vol. 178, 2020, pp. 1–14. doi:10.1016/j.actaastro.2020.08.020.

[3] Zhong, C., Chen, Z., and Guo, Y., "Attitude control for flexible spacecraft with disturbance rejection," *IEEE Transactions on Aerospace and Electronic Systems*, Vol. 53, No. 1, 2017, pp. 101–110. doi:10.1109/TAES.2017.2649259.

[4] Gennaro, S. D., "Output attitude tracking for flexible spacecraft," *Automatica*, Vol. 38, No. 10, 2002, pp. 1719–1726. doi:10.1016/S0005-1098(02)00082-1.

[5] Hu, Q., and Ma, G., "Variable structure control and active vibration suppression of flexible spacecraft during attitude maneuver," *Aerospace Science and Technology*, Vol. 9, No. 4, 2005, pp. 307–317. doi:10.1016/j.ast.2005.02.001.

[6] D'Eleuterio, G., and Hughes, P., "Dynamics of gyroelastic continua," *Journal of Applied Mechanics*, Vol. 51, No. 2, 1984, pp. 415–422. doi:10.1115/1.3167634.

[7] D'Eleuterio, G., and Hughes, P. C., "Dynamics of gyroelastic spacecraft," *Journal of Guidance, Control, and Dynamics*, Vol. 10, No. 4, 1987, pp. 401–405. doi:10.2514/3.20231.

[8] Damaren, C., and D'Eleuterio, G., "Optimal control of large space structures using distributed gyricity," *Journal of Guidance, Control, and Dynamics*, Vol. 12, No. 5, 1989, pp. 723–731. doi:10.2514/3.20467.

[9] Damaren, C., and D'Eleuterio, G., "Controllability and observability of gyroelastic vehicles," *Journal of Guidance, Control, and Dynamics*, Vol. 14, No. 5, 1991, pp. 886–894. doi:10.2514/3.20728.

[10] Hu, Q., Jia, Y., and Xu, S., "Adaptive suppression of linear structural vibration using control moment gyroscopes," *Journal of Guidance, Control, and Dynamics*, Vol. 37, No. 3, 2014, pp. 990–996. doi:10.2514/1.62267.

[11] Hu, Q., and Zhang, J., "Attitude control and vibration suppression for flexible spacecraft using control moment gyroscopes," *Journal of Aerospace Engineering*, Vol. 29, No. 1, 2016, p. 04015027. doi:10.1061/(asce)as.1943-5525.0000513.

[12] Hu, Q., Jia, Y., Hu, H., Xu, S., and Zhang, J., "Dynamics and modal analysis of gyroelastic body with variable speed control moment gyroscopes," *Journal of Computational and Nonlinear Dynamics*, Vol. 11, No. 4, 2016, p. 044506. doi:10.1115/1.4033438.

[13] Hu, Q., Jia, Y., and Xu, S., "Recursive dynamics algorithm for multibody systems with variable-speed control moment gyroscopes," *Journal of guidance, control, and dynamics*, Vol. 36, No. 5, 2013, pp. 1388–1398. doi:10.2514/1.59070.

[14] Guo, J., Geng, Y., Wu, B., and Kong, X., "Vibration suppression of flexible spacecraft during attitude maneuver using CMGs," *Aerospace Science and Technology*, Vol. 72, 2018, pp. 183–192. doi:10.1016/j.ast.2017.11.005.

[15] Guo, J., Damaren, C. J., and Geng, Y., "Space Structure Vibration Suppression Using Control Moment Gyroscope Null Motion," *Journal of Guidance, Control, and Dynamics*, Vol. 42, No. 10, 2019, pp. 2272–2278. doi:10.2514/1.g004344.

[16] Hu, Y., Geng, Y., and Wu, B., "Flexible Spacecraft Vibration Suppression by Distributed Actuators," *Journal of Guidance, Control, and Dynamics*, Vol. 43, No. 11, 2020, pp. 2141–2147. doi:10.2514/1.G005190.

[17] Hu, Y., Geng, Y., and Biggs, J. D., "Simultaneous Spacecraft Attitude Control and Vibration Suppression via Control Allocation," *Journal of Guidance, Control, and Dynamics*, Vol. 44, No. 10, 2021, pp. 1853–1861. doi:10.2514/1.G005834.

[18] Chang, H., Huang, P., Zhang, Y., Meng, Z., and Liu, Z., "Distributed control allocation for spacecraft attitude takeover control via cellular space robot," *Journal of Guidance, Control, and Dynamics*, Vol. 41, No. 11, 2018, pp. 2499–2506. doi:10.2514/1.G003626.

[19] Liu, W., Geng, Y., Wu, B., and Biggs, J. D., "Distributed Constrained Control Allocation for Cellularized Spacecraft Attitude Control System," *Journal of Guidance, Control, and Dynamics*, Vol. 45, No. 2, 2022, pp. 385–393. doi:10.2514/1.G006266.

[20] Chang, T.-H., Nedić, A., and Scaglione, A., "Distributed constrained optimization by consensus-based primal-dual perturbation method," *IEEE Transactions on Automatic Control*, Vol. 59, No. 6, 2014, pp. 1524–1538. doi:10.1109/TAC.2014.2308612.

[21] Xu, Y., Han, T., Cai, K., Lin, Z., Yan, G., and Fu, M., "A distributed algorithm for resource allocation over dynamic digraphs," *IEEE Transactions on Signal Processing*, Vol. 65, No. 10, 2017, pp. 2600–2612. doi:10.1109/TSP.2017.2669896.

[22] Nedić, A., and Ozdaglar, A., "Subgradient methods for saddle-point problems," *Journal of optimization theory and applications*, Vol. 142, No. 1, 2009, pp. 205–228. doi:10.1007/s10957-009-9522-7.

[23] Cai, K., and Ishii, H., "Average consensus on general strongly connected digraphs," *Automatica*, Vol. 48, No. 11, 2012, pp. 2750–2761. doi:10.1016/j.automatica.2012.08.003.